International Journal of Thermophysics, Vol. 21, No. 5, 2000

Two-Phase Isochoric Heat Capacity Measurements for Nitrogen Tetroxide in the Critical Region and Yang–Yang Relation

N. G. Polikhronidi,[1] R. G. Batyrova,[1] and I. M. Abdulagatov[1–3]

Received April 25, 2000

The two-phase isochoric heat capacity of nitrogen tetroxide was measured in the temperature range from 261.74 K to the critical temperature (431.072 K) at densities between 201.21 and 1426.5 $kg \cdot m^{-3}$ using a high-temperature and high-pressure adiabatic calorimeter. The measurements were performed in the two-phase region for 26 isochores (15 liquid and 11 vapor densities) including the coexistence curve and critical region. Uncertainties of the measurements are estimated to be 2%. The original temperatures and C_V data were converted to the *ITS-90*. The liquid and vapor two-phase isochoric heat capacities, temperatures, and densities at saturation were extracted from experimental data for each measured isochore. From measured (T_S, ρ_S, C'_{V2}, C''_{V2}) data, the values of second temperature derivatives of vapor-pressure d^2P_S/dT^2 and chemical potential $d^2\mu/dT^2$ were derived using the Yang–Yang relation. The results were compared with values calculated from other vapor-pressure equations. The values of saturated densities and critical parameters derived in calorimetric experiments were compared with literature data. The unusual temperature behavior of d^2P_S/dT^2 and $d^2\mu/dT^2$ was found at low temperatures around 351 K and near the critical point.

KEY WORDS: chemical potential; coexistence curve; critical point; isochoric heat capacity; nitrogen tetroxide; vapor-pressure curve.

[1] Institute of Physics of the Dagestan Scientific Center of the Russian Academy of Sciences, Kalinina 39-A, Dagestan, 367030 Makhachkala, Russia.

[2] Present address: Physical and Chemical Properties Division, National Institute of Standards and Technology, 325 Broadway, Boulder, Colorado 80303.

[3] To whom correspondence should be addressed.

0195-928X/00/0900-1073$18.00/0

1. INTRODUCTION

Nitrogen tetroxide is widely used as an oxidizer for small rockets, as an agent in heat transfer problems [1], and as a working fluid for gas-cooling atomic electric power stations [2].

The thermodynamic properties of nitrogen tetroxide are of interest not only for practical applications but for theoretical analysis. For example, two-phase isochoric heat capacity measurements along isotherms as a function of specific volume are very important for studying the strength $R\mu$ of the anomaly (Yang–Yang anomaly in fluid criticality) of second temperature derivatives of vapor-pressure d^2P_S/dT^2 and chemical potential $d^2\mu/dT^2$ near the critical point [3, 4]. The strength of the Yang–Yang anomaly $R\mu$ was first defined by Fisher [4] as $R\mu = A\mu/(A\mu + A_P)$, where $A\mu$ and A_P are the amplitudes of the singularity of $T(d^2\mu/dT^2) \approx A\mu t^{-\alpha}$ and $TV_C(d^2P_S/dT^2) \approx A_P t^{-\alpha}$.

The development of a theoretical understanding of this system which can be used as the basis for development of accurate thermodynamic predictions and correlation methods for chemically reacting systems is thus of considerable importance. Isochoric heat capacity measurements of a chemically reacting system like N_2O_4 are very important because calorimetric measurements, as compared with PVT measurements, are very sensitive to weak thermal effects of reactions $N_2O_4 \leftrightarrow 2NO_2 \leftrightarrow 2NO + O_2$. The extent of these reactions depends on both density and temperature and, therefore, the equilibrium concentration of the various components changes with temperature and density. It is also of fundamental importance to the understanding of the chemical reaction effect on the thermodynamic behavior of dissociating systems. Some experimental aspects of thermophysical property measurements on chemically reacting systems have been discussed by Bruno and Straty [5] and by Straty et al. [6].

Isochoric heat capacity C_V data are also useful to establish an equation of state because they contain information on second temperature derivatives of pressure $(\partial^2 P/\partial T^2)_\rho$ in the single-phase region and also on the first dP_S/dT and second d^2P_S/dT^2 temperature derivatives of the vapor-pressure curve. An accurate fundamental equation of state which should describe all thermodynamic properties within their experimental uncertainties can only be based on precise and thermodynamically consistent data. This equation, where the parameters are determined from PVT measurements, in general, does not yield a good representation for caloric properties (C_V, C_P, H, S) because the calculation depends upon the first and second derivatives $(\partial P/\partial T)_\rho$ and $(\partial^2 P/\partial T^2)_\rho$ of the P-T isochores. Two-phase isochoric heat capacity C_{V2} measurements are useful in developing equations for the vapor-pressure curve because they yield valuable information about

the temperature dependence of the second derivative of the pressure, (d^2P_S/dT^2), and of the chemical potential, $(d^2\mu/dT^2)$, with respect to temperature near the critical point.

Previously [7, 8], the C_V data of nitrogen tetroxide were published for five liquid isochores between 806.45 and 1426.53 $kg \cdot m^{-3}$. Recently [9] we have measured one-phase isochoric heat capacity for nitrogen tetroxide in the temperature range from 410 to 480 K, at densities between 201.21 and 980.39 $kg \cdot m^{-3}$, and for pressures up to 35 MPa. In this work, we present the new results of C_V measurements of nitrogen tetroxide in the temperature range from 261.74 K to the critical temperature (431.072 K), at densities between 201.21 and 1426.5 $kg \cdot m^{-3}$, using a high-temperature, high-pressure, and nearly constant-volume adiabatic calorimeter. These regions include two-phase liquid and vapor saturation as well as the critical region. A more detailed review of available experimental thermodynamic data for nitrogen tetroxide is presented by McCarty et al. [1].

2. ISOCHORIC HEAT CAPACITY OF FLUIDS—THERMODYNAMIC BACKGROUND

The isochoric heat capacity is one of the important fundamental thermodynamic properties of fluids and fluid mixtures. The isochoric heat capacity is directly linked with temperature derivatives of basic thermodynamic functions as follows:

$$C_{\mathbf{v}} = T\left(\frac{\partial S}{\partial T}\right)_{\mathbf{v}}, \quad C_{\mathbf{v}} = \left(\frac{\partial U}{\partial T}\right)_{\mathbf{v}}, \quad Cp = C_V + T\left(\frac{(\partial P/\partial T)_V^2}{(\partial P/\partial V)_T}\right)$$

$$W = \sqrt{-V^2 \frac{C_P}{C_V}\left(\frac{\partial P}{\partial V}\right)_T}, \tag{1}$$

$$C_{\mathbf{v}} = = -T\left(\frac{\partial^2 A}{\partial T^2}\right)_{\mathbf{v}}, \quad \left(\frac{\partial C_{\mathbf{v}}}{\partial V}\right)_{\mathbf{T}} = T\left(\frac{\partial^2 P}{\partial T^2}\right)_{\mathbf{v}}$$

where P is the pressure, A is the Helmholtz free energy, W is the speed of sound, C_p is the isobaric heat capacity, U is the internal energy, and S is the entropy.

Figure 1 show a schematic representation of the general behavior of the isochoric heat capacity C_V as a function of specific volume V for a subcritical isotherm ($T < T_C$) in the vapor (one-phase), liquid (one-phase), and vapor-liquid (two-phase) regions.

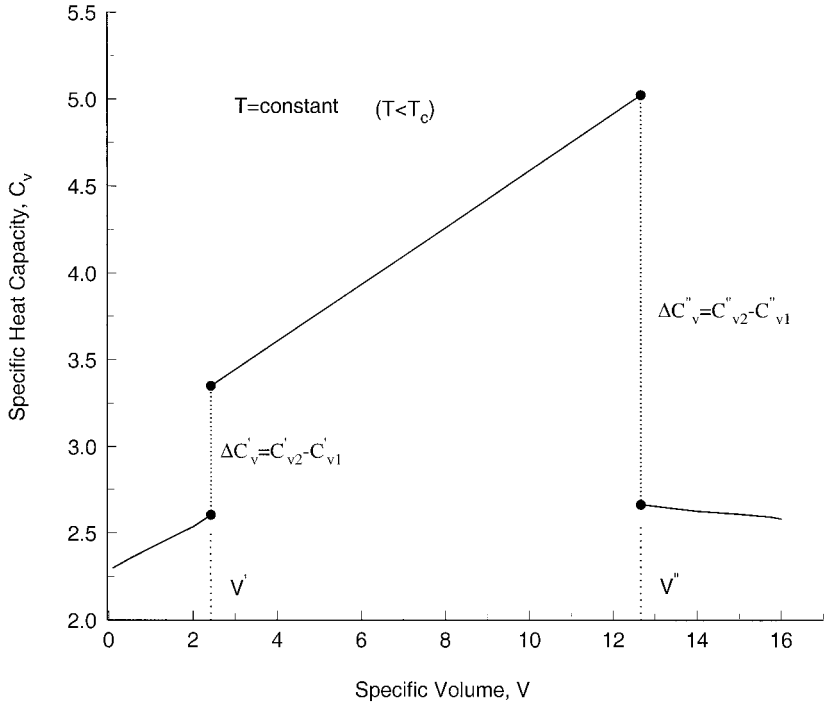

Fig. 1. Schematic representation of the general behavior of C_V as a function of specific volume V along a fixed sub-critical isotherm in the single-phase vapor, single-phase liquid, and two-phase vapor-liquid regions.

2.1. Second Temperature Derivatives d^2P_S/dT^2 and Vapor-Pressure Equation from Two-Phase Isochoric Heat Capacity Measurements

The liquid (C'_{V2}) and vapor (C''_{V2}) two-phase saturated heat capacities (see Fig. 1) are related to the second temperature derivatives of vapor-pressure (d^2P_S/dT^2) by:

$$\frac{d^2P_S}{dT^2} = \frac{C''_{V2} - C'_{V2}}{T(V'' - V')} \tag{2}$$

where V'' and V' are the vapor and liquid specific volumes at saturation, respectively, at a given temperature T.

The vapor-pressure equation from isochoric heat capacity measurements is

$$P_S(T) = P_C + \left(\frac{dP_S}{dT}\right)_C (T - T_C) + \int_{T_C}^{T} dT \int_{T_C}^{T} \frac{C''_{V2} - C'_{V2}}{T(V'' - V')}\, dT \tag{3}$$

where $(dP_S/dT)_C$ is the value of the first temperature derivative of the vapor pressure at the critical point, P_C is the critical pressure, and $\Delta P_S(T) = \int_{T_C}^{T} dT \int_{T_C}^{T} [(C''_{V2} - C'_{V2})/T(V'' - V')]\, dT$ is the curvature of the vapor-pressure curve which can be calculated using $(C'_{V2}, C''_{V2}, V'', V', T)$ measurements at saturation. The vapor-pressure curvature $\Delta P_S(T)$ has a temperature dependence of $t^{2-\alpha}$, which means that it remains finite at the critical point, but its second temperature derivative diverges weakly $d^2P_S/dT^2 \propto t^{-\alpha}$. This $(2-\alpha)$ anomaly is very difficult to detect in P_S–T_S experiments and is sometimes ignored. If, however, measurements of the two-phase C_{V2} are available, the use of the well known thermodynamic relation, Eq. (3), can yield an equation for the vapor-pressure curve which is capable of reproducing caloric (C_V, C_P, S, H) and thermal $(P_S$–$T_S)$ properties within the experimental uncertainty of the measurements. Together with the $(P_S$–$T_S)$ data, the $(C_V VT)$ measurements will provide a basis for developing new improved equations for the vapor-pressure curve which correctly take into account the nonclassical behavior of the isochoric heat capacity and can be used to test predictive models. With vapor-pressure $(P_S$–$T_S)$ data far from the critical point and $(C'_{V2}, C''_{V2}, V'', V', T)$ measurements at saturation, one can use Eq. (3) to predict values of the critical pressure P_C and the slope of the vapor-pressure curve at the critical point $(dP_S/dT)_C$ from the intercept and slope of the experimental $P_S^{\exp}(T) - \Delta P_S(T)$ vs. T, curve, respectively. The linearity of the experimental behavior of $P_S^{\exp}(T) - \Delta P_S(T)$ can be used as a criterion to determine the consistency the independent thermal $(P_S$–$T_S)$ and caloric $(C_V VT)$ measurements at saturation.

2.2. Two-Phase Isochoric Heat Capacity and Behavior of the Second Temperature Derivatives of the Chemical Potential $(d^2\mu/dT^2)$

At coexistence, the relation of Yang and Yang [10] is

$$\frac{C_{V2}}{T} = -\frac{d^2\mu}{dT^2} + V\frac{d^2P_S}{dT^2} \tag{4}$$

where C_{V2} is the two-phase isochoric heat capacity and V is the specific volume.

According to Eq. (4), the two-phase isochoric heat capacity C_{V2} is a linear function of the specific volume V along each isotherm, the slopes of which equal $T(d^2P_S/dT^2)$ while the intercepts for $V=0$ are related to $-T(d^2\mu/dT^2)$.

From Eq. (4) for the second temperature derivative of the chemical potential $d^2\mu/dT^2$ we can write

$$\frac{d^2\mu}{dT^2} = \frac{V''C'_{\mathbf{V2}} - V'C''_{\mathbf{V2}}}{T(V' - V'')} \tag{5}$$

Thus, Eqs. (2) and (5) which relate second temperature derivatives of the vapor-pressure curve $P_S(T)$ and chemical potential $\mu(T)$ with values of two-phase isochoric heat capacities at saturation ($C'_{\mathbf{V2}}$, $C''_{\mathbf{V2}}$), saturated liquid and vapor specific volumes (V', V''), and saturated temperature $T_S(V)$ provide a very sensitive test to the internal consistency between these properties measured in the same experiments. Even small variations or inconsistencies between ($C'_{\mathbf{V2}}$, $C''_{\mathbf{V2}}$) and (V', V'', T) measurements result in significant differences in the derived properties d^2P_S/dT^2 and $d^2\mu/dT^2$. Apparently good agreement between measurements and calculated values of C_V may not signify reliability of these data. Therefore, Eqs. (2) and (5) can be used as sensitive criteria for testing the internal consistency between (C'_{V2}, C''_{V2}, V'', V', T) quantities and independent vapor-pressure measurements $P_S(T)$. These criteria are also very useful to test the accuracy of the vapor-pressure equations and accuracy of (C'_{V2}, C''_{V2}, V'', V', T) properties.

3. EXPERIMENTAL

Details of the construction of the calorimeter and experimental procedures are given in several papers [9, 11–15]. The calorimeter is a multilayered system which consists of an internal thin-walled vessel, outer adiabatic shells, and a semiconductor layer (cuprous oxide) of 2 mm thickness between the shells. The inner vessel was constructed from heat- and corrosion-resistant high-strength stainless steel (1X18H9T) with walls 1.0 mm thick. Cylindrical wells are used for an internal heater, resistance thermometer, and measuring thermocouples. The outer shell is made of the same steel, but has walls 6 to 8 mm in thickness.

The heat capacity of the empty calorimeter C_0 was determined using standard substances (*n*-heptane and helium) with well-known isobaric heat capacities [16], in the temperature range up to 473 K along isochores 465.12 and 142.25 $\mathrm{kg \cdot m^{-3}}$ for *n*-heptane, and 20.121 $\mathrm{kg \cdot m^{-3}}$ for helium. The uncertainties of the C_P data used for calibration are 0.5% for *n*-heptane and 0.1% for helium. The results of these measurements of C_0 can be described by the equation

$$C_0 = 167.1 + 0.1T$$

where T (in K) is the temperature and C_0 (in $J \cdot K^{-1}$) is the empty calorimeter heat capacity. This equation reproduced experimental values of C_0 within $\pm 0.9\%$. The empty calorimeter heat capacity C_0 depends also on the scanning rate. Using various standard fluids with different thermophysical characteristics the optimal rate of scanning was determined such that values of C_0 are reproduced within an uncertainty of 1 to 2 $J \cdot K^{-1}$. As a rule, the rate of scanning falls within a narrow range of about (0.5 to 8) $\times 10^{-4}$ $K \cdot s^{-1}$.

At a given temperature and atmospheric pressure, the volume of the calorimeter can be found from the density of water [17]. Five to six repetitions at different temperatures were used in each experiment. The uncertainty in determining the working volume of the calorimeter did not exceed 0.05%. Changes in the volume of the calorimeter due to changes in temperature (ΔV_T) and pressure (ΔV_P) were determined both experimentally and by calculation as

$$\Delta V_T = 4.9980 \times 10^{-5} \Delta T + 17.7777 \times 10^{-9} \Delta T^2, \quad \Delta V_P = 10^{-5}(1.775P - 2.5)$$

where $\Delta V_T = V_T - V_O$; $\Delta V_p = V_P - V_O$; and $V_O = 440.43 \pm 0.05$ cm^3 is the volume of the calorimetric vessel at 296.65 K and atmospheric pressure 0.101325 MPa.

At the maximum pressure ($P = 35$ MPa), the correction for the pressure dilation was 0.62 cm^3. The uncertainties in the determination of ΔV_T and ΔV_P are 2.1 and 13%, respectively. Therefore, the uncertainties in the determination of the calorimeter volume with corrections for ΔV_T and ΔV_P is $\pm 0.05\%$ or ± 0.2 cm^3 in the temperature range from 410 to 485 K.

Measurements of C_V were carried out at constant volume by the continuous-heating method. This method enables one to determine the transition temperature T_s of the system from the two-phase to a single-phase state (i.e., to determine T_s and ρ_s data corresponding to the coexistence curve), the jump in the heat capacity ΔC_V, and reliable C_V data in the single- and two-phase regions. The techniques of determining parameters T_s and ρ_s at the coexistence curve and measuring the heat capacity C_V at this curve are similar to the method of quasi-static thermograms described by Chashkin et al. [18] and by Voronel [19]. In comparison with the technique described by Chashkin et al. [18] and by Voronel [19], the method of thermograms ($T - \tau$ plot) here is supplemented by recording readings of the sensor of adiabaticity; in combination, these ensure sufficient information on the changes in the sample thermodynamic state. On intersecting the phase transition curve, the heat capacity is known to jump, leading to a sharp change in the thermogram slope ($dT/d\tau$). The high

sensitivity of cuprous oxide makes it possible to fix immediately the temperature changes on a strip-chart recorder. Measurements near the phase transition are usually carried out using temperature cycling, i.e., heating (forward direction, $dT/d\tau > 0$) and cooling (reverse direction, $dT/d\tau < 0$). The system for such cycling goes from a two-phase state to a single-phase state or vice versa.

The method under consideration makes it possible to obtain reliable data up to temperatures of $T_c \pm 0.01$ K. At the phase transition point, the slope of the thermograms changes by 20–30% on average along an isochore, which makes it possible to easily determine the transition temperature. The rate of temperature change, determined by the power supplied to the internal heater, varied from $(1\text{–}2) \times 10^{-3}$ (far from the critical point) to 5×10^{-5} K $\cdot$ s^{-1} (in the critical region). Near the critical point and the phase transition curve, the measurements were performed using minimal rates. All measurements were made with the samples stirred by a thin perforated steel foil at a frequency of 1 Hz. This accelerates the equilibration of the system near the critical point.

In the region of normal behavior of C_V, the measurements were carried out in temperature steps of 0.1 to 0.2 K; in the region of critical anomalies, the step was decreased to 0.02 K. The heat capacity C_V is calculated by the expression

$$C_V = \frac{1}{m}\left\{\frac{\Delta Q}{\Delta T} - C_0\right\} \tag{6}$$

where m is the mass of the sample in the calorimeter, $\Delta Q = IU\tau$ is the heat released by the internal heater, I is the current passing through the internal heater, U is the voltage drop, τ is the heating time, and C_0 is the heat capacity of the empty calorimeter.

The heat capacity was obtained from the measured quantities m, I, U, τ, ΔT, and C_0. The accuracy of the heat capacity measurements was assessed by analyzing the sensitivity of Eq. (6) to the experimental uncertainties of the measured quantities.

The temperature was measured with a *PRT* (*PTS-10*) mounted in a tube inside the calorimetric sphere. The thermometer was calibrated on *IPTS-68*. The uncertainty of the temperature measurements was less than 10 mK. The density of the sample was determined as the ratio of the mass of the sample m to the working volume V_{PT} of the calorimetric vessel, $\rho = m/V_{PT}$.

The correction related to the nonisochoric behavior during heating was determined to an uncertainty of 9.5% on the isochore 1426.53 kg $\cdot$ m^{-3} and 4.0% on the isochore 200.00 kg $\cdot$ m^{-3}. The standard deviation for this

correction $C_V - C_V^{\exp}$ is 11%. The absolute uncertainty in C_V due to not reaching an adiabatic condition is 0.013 $kJ \cdot K^{-1}$. The maximum uncertainty in the experimentally determined C_V resulting from the absolute uncertainties of the specific volume $\Delta V = 4 \times 10^{-4} V$ and temperature $\Delta T = 0.01$ K is 0.16% near the phase transition points (in the lower range $T - T_S = 0.5$ K) and 0.05% in the range far from phase transition points. Thus, the combined standard uncertainty related to the indirect character of measurements did not exceed 0.16%.

Surface temperature gradients of about 0.1 $K \cdot m^{-1}$ would result in systematic uncertainties in the measured C_V up to 5%. To minimize these gradients, all thermal screens were made from copper and controlled with additional heaters. The control of the surface temperature gradients was achieved using differential copper-constantan thermocouples. This permits reduction of the temperature gradients on the surface of the calorimeter vessel to a level of 0.02 $K \cdot m^{-1}$. The time to reach equilibrium when the state conditions are changed is 10^{-6} s; therefore, the effect on the equilibrium of the process is negligibly small.

Based on the detailed analysis of all sources of uncertainties likely to affect the determination of C_V with the present system, the combined standard uncertainty of measuring the heat capacity with an allowance for the uncertainty related to the nonisochoric conditions was 2%.

The purity of the nitrogen tetroxide was 99.3% by mass. The impurities were 0.4% by mass NO, 0.2% by mass HNO_3, and 0.07% by mass N_2. Before and after the measurements, the sample of N_2O_4 for each isochore was analyzed in the Institute Nuclear Energy (Minsk, Belarus) by a chromatographic method. For some low-density isochores between 201.21 and 238.10 $kg \cdot m^{-3}$, where the impurity reached 0.5% by mass NO and 0.32% by mass HNO_3, we found a change of sample composition. This changes were probably caused by contact with the atmosphere ($N_2O_4 + H_2O \rightarrow HNO_3$). Under the conditions of the experiment, the reaction is reversible. The relaxation time of the reaction $N_2O_4 \leftrightarrow 2NO_2$ is about 10^{-8} s.

4. RESULTS AND DISCUSSION

Measurements of the isochoric heat capacity for nitrogen tetroxide (N_2O_4) were performed along 26 isochores, namely, 201.05, 234.69, 326.62, 400.58, 454.57, 500.50, 521.11, 527.93, 539.84, 545.02, 549.75, 562.46, 569.64, 575.37, 578.50, 605.03, 631.03, 682.50, 798.28, 804.70, 897.75, 983.48, 998.10, 1186.80, 1338.50, and 1426.50 $kg \cdot m^{-3}$. The temperature range was 261.74 K to the critical temperature (431.072 K). In total, 291 C_V measurements was made in the two-phase region. A total of 56 values

Table I. Experimental Values of the Two-Phase Isochoric Heat Capacities of Nitrogen Tetroxide (N_2O_4)

T (K)	C_V (kJ · kg^{-1} · K^{-1})
$\rho = 1426.5$ kg · m^{-3}	
261.738	1.554
261.859	1.556
265.620	1.583
266.429	1.578
270.875	1.537
271.414	1.535
278.835	1.575
279.360	1.582
284.975	1.547
285.428	1.580
290.264	1.576
293.820	1.571
294.593	1.575
295.064	1.572
300.512	1.599
300.815	1.603
301.053	1.607
$\rho = 1338.5$ kg · m^{-3}	
262.700	1.546
266.970	1.546
267.420	1.547
273.654	1.562
278.863	1.547
279.792	1.563
280.354	1.572
285.816	1.567
290.906	1.565
292.508	1.600
295.611	1.603
301.409	1.619
306.885	1.649
308.646	1.636
318.196	1.713
328.342	1.764
334.523	1.817
$\rho = 1186.8$ kg · m^{-3}	
269.680	1.550
273.728	1.554
274.250	1.555
278.827	1.554
279.142	1.557
283.527	1.572
288.518	1.571
297.572	1.625
298.556	1.579
307.512	1.653
318.480	1.735
328.612	1.779
334.568	1.819
345.040	1.994
358.406	2.134
359.811	2.149
362.828	2.244
368.746	2.388
372.648	2.508
374.666	2.474
375.484	2.522
377.660	2.545
379.378	2.602
380.289	2.638
$\rho = 998.1$ kg · m^{-3}	
274.382	1.600
277.695	1.591
278.142	1.571
283.328	1.583
286.329	1.588
292.188	1.634
294.514	1.639
324.496	1.702
324.951	1.675
333.279	1.821
333.540	1.815
343.626	2.007
353.830	2.102
354.150	2.096
368.835	2.316
410.669	3.758
411.642	3.781
412.470	3.800
412.886	3.797
$\rho = 983.5$ kg · m^{-3}	
333.982	1.929
362.693	2.345
387.778	2.956
411.008	3.963
412.262	3.955
412.923	3.989
413.429	4.004
413.720	4.006
413.820	4.041
$\rho = 897.7$ kg · m^{-3}	
312.030	1.739
337.499	1.864
359.542	2.131
379.511	2.564
394.633	3.032
408.185	3.562
419.930	4.352
421.063	4.565
421.784	4.652
$\rho = 804.7$ kg · m^{-3}	
273.561	1.619
283.359	1.648
292.518	1.634
293.268	1.648
293.585	1.645
297.480	1.648
312.358	1.685
325.530	1.775
335.766	1.866
373.673	2.540
374.314	2.559
391.905	3.144
403.013	3.727
413.844	4.493
427.212	5.812
427.327	5.834
$\rho = 798.3$ kg · m^{-3}	
314.478	1.755
326.050	1.820

Table I. *(Continued)*

T (K)	C_V (kJ · kg^{-1} · K^{-1})	T (K)	C_V (kJ · kg^{-1} · K^{-1})	T (K)	C_V (kJ · kg^{-1} · K^{-1})
341.110	2.050	403.667	4.264	$\rho = 539.8$ kg · m^{-3}	
357.060	2.312	410.694	4.778	430.913	10.500
372.610	2.687	413.512	5.160	430.995	10.769
389.280	3.225	419.930	5.812	431.015	11.632
404.300	3.985	420.030	5.750	431.036	12.200
418.693	4.824	428.344	7.462	431.056	13.026
427.124	5.939	430.384	8.704		
		430.935	10.200	$\rho = 549.8$ kg · m^{-3}	
$\rho = 682.5$ kg · m^{-3}				430.975	10.840
		$\rho = 569.6$ kg · m^{-3}		430.995	11.090
312.280	1.726			431.015	11.543
326.290	1.822	414.552	5.118	431.036	11.958
337.270	1.961	423.532	6.309	431.056	12.910
350.350	2.186	430.486	8.780		
364.262	2.520	430.792	9.600	$\rho = 527.9$ kg · m^{-3}	
375.590	2.814	430.883	10.140		
395.600	3.629			413.876	5.269
413.620	4.757	$\rho = 578.5$ kg · m^{-3}		419.364	6.005
422.608	5.679			425.942	7.054
430.180	7.980	430.456	8.600	430.954	10.920
430.384	8.100	430.762	9.350	431.015	11.810
		430.925	10.084	431.036	12.300
$\rho = 631.0$ kg · m^{-3}		430.966	10.388	431.056	13.250
		431.007	11.906		
423.640	6.102	431.027	11.353	$\rho = 521.1$ kg · m^{-3}	
427.220	6.864				
429.874	7.557	$\rho = 562.5$ kg · m^{-3}		430.689	9.630
430.282	7.967			430.954	11.186
430.690	8.735	430.558	9.001	430.975	11.400
		430.762	9.540	431.015	12.053
$\rho = 605.0$ kg · m^{-3}		430.925	10.310	431.036	12.446
		430.966	10.640		
425.318	6.497	431.007	11.091	$\rho = 500.5$ kg · m^{-3}	
430.384	8.369	431.048	12.530		
430.588	8.818			349.544	1.989
430.894	9.910	$\rho = 545.0$ kg · m^{-3}		362.243	2.341
				371.617	2.697
$\rho = 575.4$ kg · m^{-3}		414.188	5.326	370.951	2.664
		419.724	6.024	382.801	3.208
310.310	1.411	426.095	7.035	383.344	3.232
324.855	1.580	430.333	8.863	384.755	3.294
333.810	1.711	430.913	10.440	402.929	4.536
348.113	1.943	430.954	10.834	403.351	4.522
360.285	2.257	431.015	11.580	414.240	5.553
372.500	2.670	431.036	12.060		
387.240	3.333	431.056	12.870		

Table I. *(Continued)*

T (K)	C_V (kJ·kg^{-1}·K^{-1})	T (K)	C_V (kJ·kg^{-1}·K^{-1})	T (K)	C_V (kJ·kg^{-1}·K^{-1})
424.250	7.001	427.372	8.760	413.840	8.910
430.750	10.333	428.037	9.419	417.630	9.705
430.913	11.103	429.057	9.940	418.520	9.912
$\rho = 454.6$ kg·m^{-3}		$\rho = 326.6$ kg·m^{-3}		$\rho = 201.0$ kg·m^{-3}	
342.500	1.866	327.240	1.623	315.625	1.004
353.760	2.224	339.598	1.843	319.212	1.070
369.061	2.702	344.727	2.087	324.305	1.363
382.038	3.408	360.016	2.553	328.786	1.295
393.038	4.212	367.678	3.007	329.070	1.466
401.766	4.842	372.110	3.255	336.212	1.702
413.928	6.148	385.534	4.253	337.873	1.713
424.353	7.727	402.887	5.920	343.093	1.816
427.268	8.030	418.753	8.123	354.000	2.386
430.476	10.060	422.007	8.680	361.680	3.030
430.628	10.300	425.150	9.440	367.835	3.692
430.709	10.423	426.647	9.839	374.204	4.309
		427.078	9.940	376.908	4.439
$\rho = 400.6$ kg·m^{-3}				381.602	4.922
323.060	1.480	$\rho = 234.7$ kg·m^{-3}		387.240	5.630
335.630	1.667	347.705	2.003	388.530	5.735
349.320	1.954	347.837	1.919	392.503	6.323
361.568	2.408	356.270	2.332	396.161	6.630
375.370	3.204	367.500	3.260	401.151	7.438
391.430	4.252	378.550	4.278	404.342	8.359
407.450	5.630	390.357	5.455	408.855	8.931
420.342	7.269	397.524	6.439	416.406	10.375
422.027	7.460	406.190	7.444	416.623	10.810

of C_V and T_S were measured on the coexistence curve. The experimental values are given in Tables I and II and shown in Figs. 2 to 6. Each data point in Tables I and II in the range far from the coexistence curve where C_V slowly changes with temperature is the average of 10 measurements. Figure 2 shows the experimental behavior of two-phase C_{V2} as a function of temperature for N_2O_4 along selected vapor and liquid isochores. The variation of C_{V2} with specific volume V along various isotherms including near-critical isotherms is shown in Fig. 3. All isotherms show a strong almost linear dependence of C_{V2} with volume V as predicted by the Yang–Yang relation, Eq. (4). The rapidly increasing slope of the isotherms as the critical temperature is approached reflects an increase in the second temperature derivative, d^2P_S/dT^2. The measured two-phase specific

Table II. Experimental Values of the Two-Phase Isochoric Heat Capacities of Nitrogen Tetroxide (N_2O_4) Along the Saturation Boundary

T_S (K)	ρ'_S ($kg \cdot m^{-3}$)	C'_{V2} ($kJ \cdot kg^{-1} \cdot K^{-1}$)	T_S (K)	ρ''_S ($kg \cdot m^{-3}$)	C''_{V2} ($kJ \cdot kg^{-1} \cdot K^{-1}$)
301.158	1426.5	1.615	417.033	201.0	11.086
335.126	1338.5	1.829	420.802	234.7	10.650
380.584	1186.8	2.523	427.232	326.6	10.045
412.933	998.1	3.809	429.827	400.6	10.040
413.985	983.5	4.044	430.706	454.6	10.600
421.992	897.7	4.755	430.976	500.6	12.020
427.336	804.7	5.844	431.018	521.1	13.200
427.546	798.3	5.980	431.026	527.9	13.950
430.440	682.5	8.160	431.035	539.8	15.670
430.851	631.0	9.600	431.036	545.0	16.600
430.972	605.0	10.844	431.037	549.8	18.961
431.021	578.5	12.790			
431.025	575.4	13.140			
431.031	569.6	13.870			
431.036	562.5	15.130			

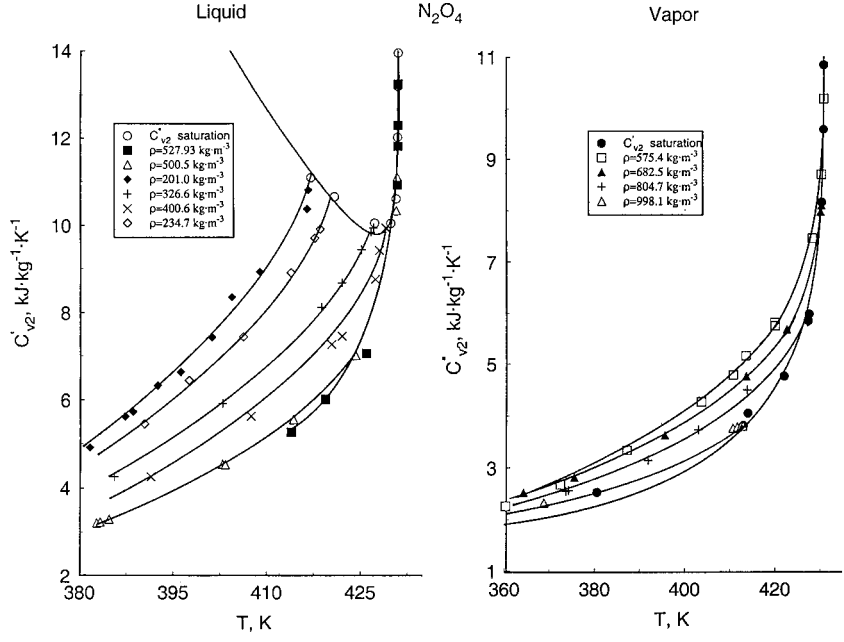

Fig. 2. Liquid (C'_{V2}) and vapor (C''_{V2}) two-phase isochoric heat capacities of nitrogen tetroxide as a function of temperature along selected isochores.

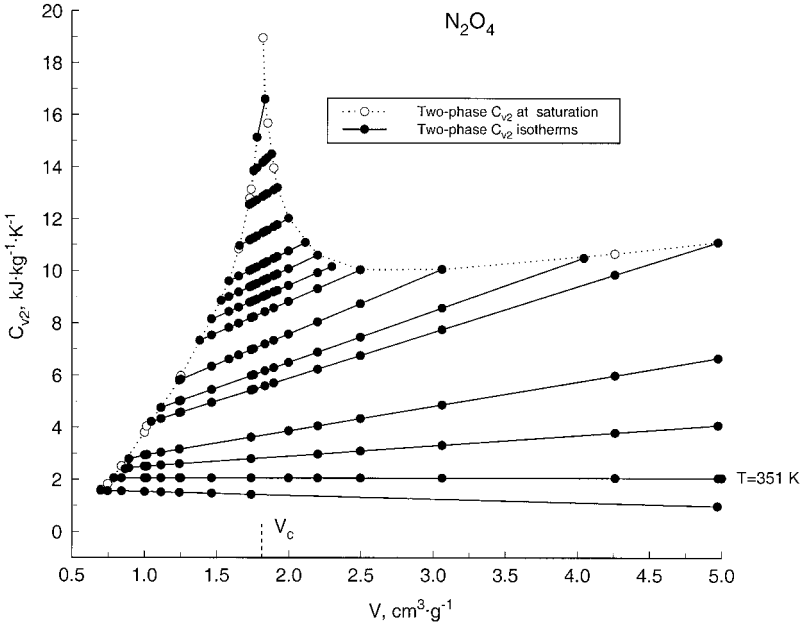

Fig. 3. Two-phase isochoric heat capacities of nitrogen tetroxide as a function of specific volume along various isotherms. For isotherm $T = 351$ K, the slope of the C_{V2}–V curve is zero.

isochoric heat capacity data at saturation (C'_{V2}, C''_{V2}) for N_2O_4 were used to derive a set of second derivatives d^2P_S/dT^2 and $d^2\mu/dT^2$. Figure 4 and Table III demonstrate the temperature dependence of the vapor-pressure derivative (d^2P_S/dT^2), derived from C_{V2} measurements for N_2O_4 using Eq. (2) together with values calculated from various vapor-pressure equations. As can be see from Fig. 3, the volume dependence of the two-phase C_{V2} along isotherms near a temperature of 351 K show unusual behavior when compared to ordinary fluids [11–14, 20, 21]. Namely, along the isotherm 351 K, C_{V2} is almost independent of the volume V; therefore, the slope of the C_{V2}–V curve along this isotherm is zero. This means that the second temperature derivative of the vapor-pressure curve at 351 K is zero, $(d^2P_S/dT^2) = 0$. Moreover, the isotherms below 351 K show negative slopes, i.e., $(d^2P_S/dT^2) < 0$. This is unusual behavior of (d^2P_S/dT^2) for chemically reacting systems like nitrogen tetroxide. For all isotherms above 351 K, the slope of the C_{V2}–V curves is positive as observed in most previous studies [11–14, 20]. This unusual behavior of the two-phase isochoric heat capacity for N_2O_4 can be explained as a result of a chemical reaction (dissociation of the molecules of N_2O_4). Indeed, the contribution

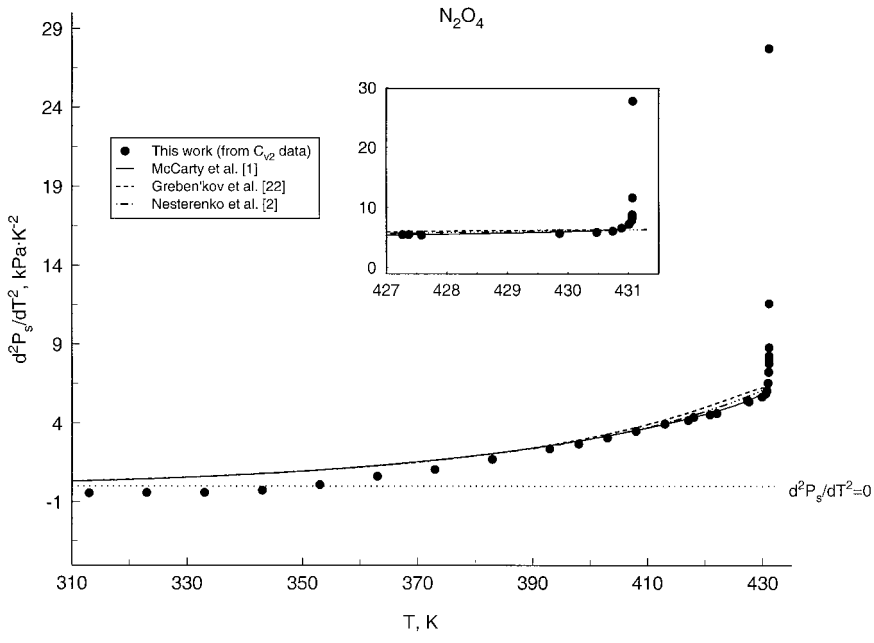

Fig. 4. Second temperature derivative of vapor-pressure curve derived from two-phase isochoric heat capacity measurements using Eq. (2) together with values calculated from vapor-pressure equations.

of the chemical reaction on the measured heat capacity on the coexistence curve can be estimated using the following equation [2]:

$$C'_{\mathrm{Vrea}} = \alpha' \frac{dq}{aT} + q \frac{d\alpha'}{dT} \qquad \text{and} \qquad C''_{\mathrm{Vrea}} = \alpha'' \frac{dq}{aT} + q \frac{d\alpha''}{dT} \tag{7}$$

where $\alpha'(T)$ and $\alpha''(T)$ are the equilibrium constants of the chemical reaction on the coexistence curve; C'_{Vrea} and C''_{Vrea} are the liquid and vapor two-phase heat capacities at saturation caused by the chemical reaction. The values of the two-phase C_{Vrea} calculated using Eq. (7) for N_2O_4 along the various isotherms as a function of specific volume are shown in Fig. 5. As can be seen in this figure, C_{Vrea}–V isotherms show negative slopes which is opposite to the measured C_{V2}–V isotherms as shown in Fig. 3. Around 351 K the slopes of the C_{Vrea}–V curves change sign from negative to positive. Since there is competition between the two opposite contributions to the measured values of the two-phase heat capacities, the derivative (d^2P_S/dT^2) is affected by both chemical reactions and intermolecular

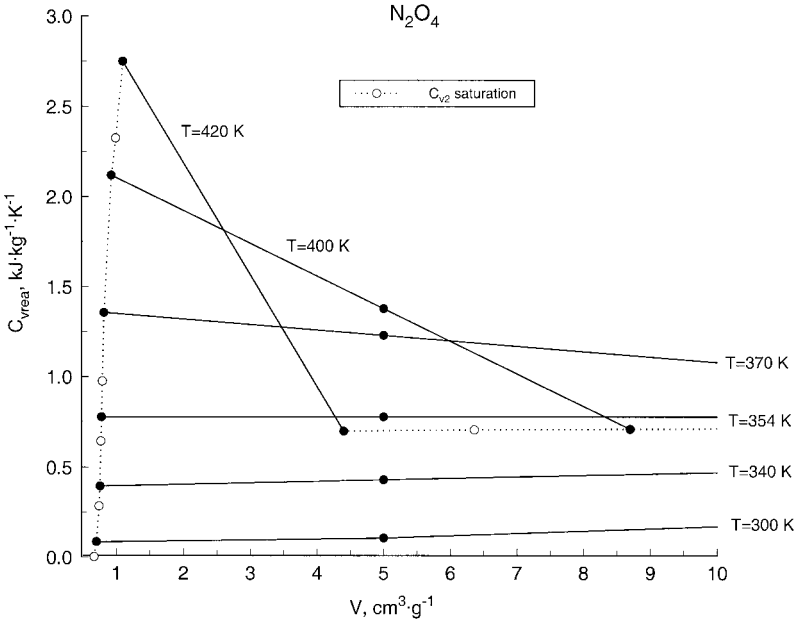

Fig. 5. Two-phase isochoric heat capacities of nitrogen tetroxide caused by chemical reaction as a function of specific volume for selected isotherms calculated from Eq. (7).

interactions. Therefore, at temperatures above 351 K, the effect of dissociation is smaller than the intermolecular interaction contribution, while at temperatures below 351 K, the effect of chemical reaction dominates the intermolecular interaction. Around 351 K, the contributions are nearly identical but with opposite sign and the measured slope of the C_{V2}–V curve is near zero. Some unusual temperature dependence of the one-phase C_V vs. T isochores was also found in our previous measurements [9] for nitrogen tetroxide.

The second temperature derivatives of the chemical potential $d^2\mu/dT^2$ calculated from our experimental C_{V2} data using Eq. (5) for N_2O_4 are given in Fig. 6 and in Table III. This figure also show the $\log(d^2\mu/dT^2)$ as a function of $\log t$ in the asymptotic range of the critical point. As shown in Fig. 6, at temperatures below 427 K, $d^2\mu/dT^2$ is almost constant, while at temperatures close to the critical point, the values of $d^2\mu/dT^2$ increase sharply, the same behavior as for the second temperature derivative of the vapor pressure. The slope of $\log(d^2\mu/dT^2)$ vs. $\log t$ curve is about 0.118 ± 0.002 which is very close to the weak singularity of C_V. This confirms the conclusion made in Refs. 3 and 4 that the singularity of C_{V2}

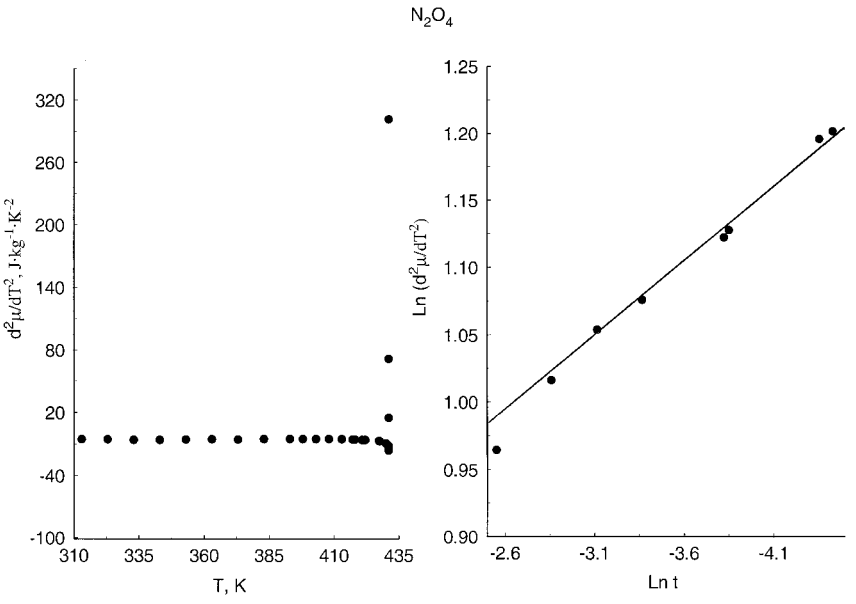

Fig. 6. Second temperature derivative of chemical potential derived from two-phase isochoric heat capacity measurements using Eq. (5).

near the critical point is shared between (d^2P_S/dT^2) and $d^2\mu/dT^2$ on the basis of a careful analysis of our previous two-phase isochoric heat capacity measurements for propane [22].

The experimental values of liquid and vapor two-phase (C'_{V2}, C''_{V2}) isochoric heat capacities on the coexistence curve are shown in Fig. 7 together with our previous one-phase (C'_{V1}, C''_{V1}) measurements at saturation [9]. The isochoric heat capacity rises to a maximum at the coexistence curve for each isochore, and then drops discontinuously to a value corresponding to the one-phase state. The magnitudes of isochoric heat-capacity jumps for liquid $(\Delta C'_V = C'_{V2} - C'_{V1})$ and vapor $(\Delta C''_V = C''_{V2} - C''_{V1})$ isochores are shown in Fig. 8 as a function of temperature. One- and two-phase isochoric heat capacities of N_2O_4 as a function of temperature for two near-critical densities are shown in Fig. 9. The heat capacity curve of N_2O_4 as a function of temperature near the phase transition temperature shows a lambda shape. For each liquid and vapor isochore, C_V measurements were made in the two-phase region at temperatures $T \leqslant T_S$, including the liquid, vapor, and near-critical states. More detail measurements were made in the critical region and near the phase transition points which are very important for determination of the shape of the coexistence curve near the critical point and of the values of the critical parameters. The

Table III. Second Temperature Derivatives (d^2P_S/dT^2) and $(d^2\mu/dT^2)$ from Two-Phase Isochoric Heat Capacities Measurements of Nitrogen Tetroxide

T_S (K)	d^2P_S/dT^2 (kPa · K^{-2})	$d^2\mu/dT^2$ (J · kg^{-1} · K^{-2})
313	−0.444	−5.340
323	−0.408	−5.601
333	−0.398	−5.913
343	−0.269	−6.007
353	0.100	−5.755
363	0.618	−5.428
373	1.061	−5.663
383	1.700	−5.155
393	2.382	−5.097
398	2.684	−5.184
403	3.076	−5.200
408	3.490	−5.258
413	3.959	−5.323
417.067	4.192	−5.729
418.000	4.385	−5.657
420.837	4.541	−5.957
422.027	4.636	−6.102
427.268	5.443	−6.845
427.372	5.436	−6.918
427.582	5.370	−7.258
429.863	5.663	−9.220
430.476	5.851	−10.383
430.742	6.038	−11.325
430.887	6.539	−11.917
431.008	7.202	−13.255
431.012	7.240	−13.422
431.054	7.773	−15.706
431.057	7.969	−15.917
431.061	8.250	−16.144
431.062	8.769	−15.752
431.067	11.580	−11.847
431.071	27.712	14.982
431.072	59.930	71.450
431.073	190.006	301.630

experimental results for temperatures T_S and densities ρ_S along the coexistence curve which were determined from C_V experiments using the method of quasi-static thermograms are presented in Table II and Fig. 10, together with values from the literature (McCarty et al. [1], Nesterenko et al. [2], and Grebenkov et al. [22]). For these data the deviations statistics

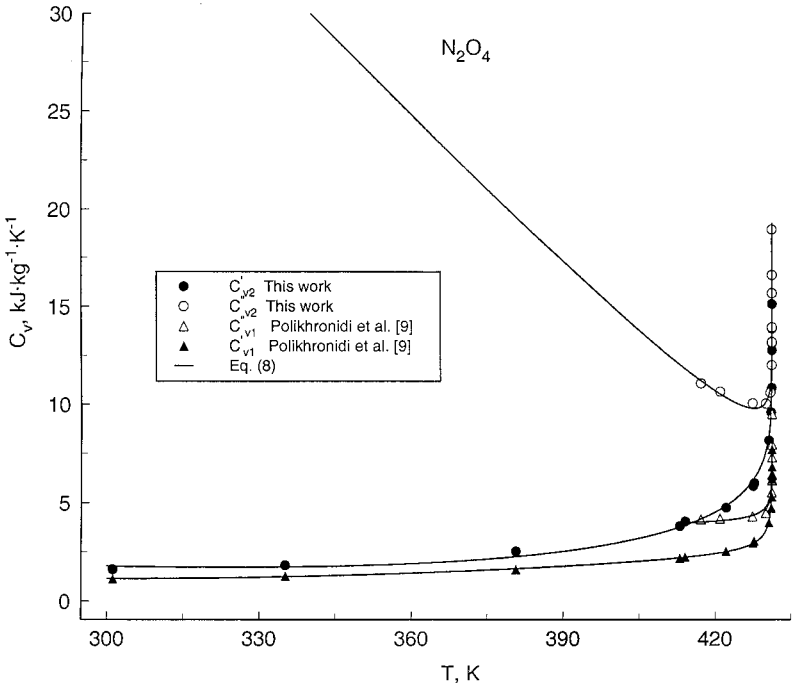

Fig. 7. Liquid and vapor two-phase and single-phase isochoric heat capacities of nitrogen tetroxide as a function of temperature along the coexistence curve.

are as follows: Nesterenko et al. [2]—AAD = 2.39%, Bias = −1.03%, St. Dev. = 3.15, St. Error = 0.67, Max. Dev. = 7.65%; McCarty et al. [1]—AAD = 2.45%; Bias = 0.25%; St. Dev. = 3.41; St. Error = 0.74, Max. Dev. = 6.68%; Grebenkov et al. [22]—AAD = 1.94%; Bias = −0.70%; St. Dev. = 2.99; St. Error = 0.86, Max. Dev. = 8.77%.

The maximum deviations appear in the immediate vicinity of the critical point. At low temperatures ($T < 422$ K) the liquid density data at saturation of Nesterenko et al. [2] show good agreement within ±0.5% of our data. For vapor density data at saturation, the Nesterenko et al. [2] results show excellent agreement within +0.3% of our C_V experiment results. But, near the critical point, the deviations reached +5.15%. All of the Grebenkov et al. [22] data for saturated liquid density show systematic negative deviations of about −0.74%, except for two data points in the immediate vicinity of the critical point at 430.478 and 431.008 K, which show deviations of about −3.07% and −8.77%, respectively. For vapor densities at saturation, the deviations are systematically positive at +1.48%, including the near-critical region. From our experimental

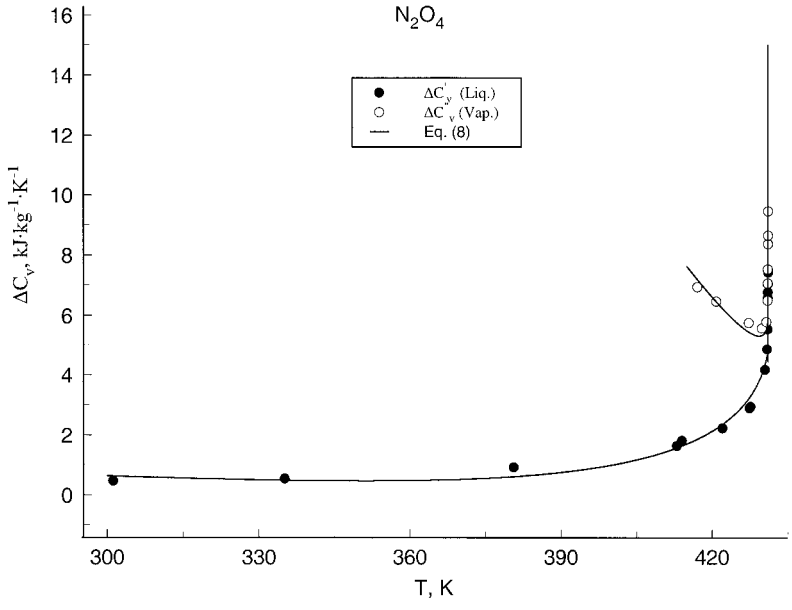

Fig. 8. Liquid ($\Delta C'_V$) and vapor ($\Delta C''_V$) isochoric heat capacity jump for nitrogen tetroxide as a function of temperature.

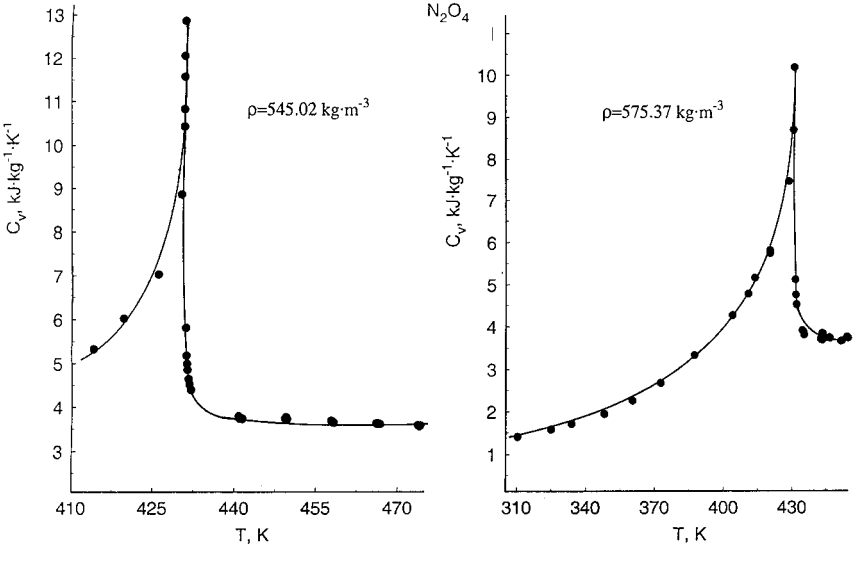

Fig. 9. Two- and single-phase isochoric heat capacities of nitrogen tetroxide as a function of temperature along selected near-critical isochores.

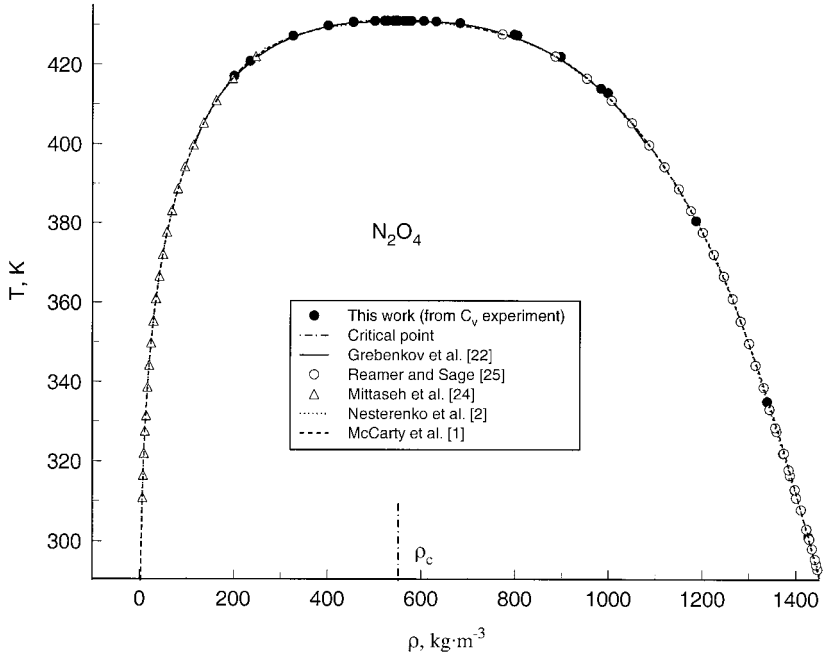

Fig. 10. Curves of coexisting liquid and vapor densities for nitrogen tetroxide from C_V experiments together with values derived from other investigations.

(T_S, ρ_S) data at saturation, we have deduced values for the critical temperature T_C and critical density ρ_C for N_2O_4. Our results of $T_C = 431.073 \pm 0.01$ K and $\rho_C = 551.70 \pm 0.05$ kg · m^{-3} are in satisfactory agreement within ± 0.2 K and $\pm 0.3\%$, respectively, with literature values (Nesternko et al. [2]—$T_C = 431.35$ K and $\rho_C = 552.75 \pm 2.75$ kg · m^{-3}; McCarty et al. [1]—$T_C = 431.372$ K and $\rho_C = 550.463$ kg · m^{-3}; Grebenko et al. [22]—$T_{C^*} = 430.95 \pm 0.04$ K and $\rho_C = 556.20 \pm 1.2$ kg · m^{-3}). The uncertainty of the critical parameters derived from our experiment do not include the impurity effect. The critical parameter values for the ternary system ($N_2O_4 + NO_2 + NO$) depend on the degree of dissociation [21].

All original experimental temperatures were converted to the *ITS-90* from the *IPTS-68* temperature scale. The corresponding values of the measured C_V data were corrected for temperature scale conversions using the relationship recommended by Rosby [23]. The effect of temperature scale differences on the C_V data is small. At temperatures below 400 K, the magnitude of the correction is about 0.0008%, and for temperatures above 400 K, the correction reached 0.027%.

Table IV. Parameters A_i for Eq. (8)

A_0	A_1	A_2	A_3	A_4	χ^2	Thermodynamic paths
3.90307	5.55331	−4.49610	−12.33226	15.60028	1.01	Single-phase C'_{V1} along coexistence line
2.37179	2.06204	0	0	0	1.58	Single-phase C''_{V1} along coexistence line
2.88128	−15.8231	3.61085	15.97700	0	1.78	Two-phase C'_{V2} along coexistence line
2.39233	−8.81498	6.05639	122.5938	0	1.62	Two-phase C''_{V2} along coexistence line

The results of the isochoric heat capacity measurements along the coexistence line were correlated by fitting the scaling type function:

$$C_V/\mathrm{kJ}\cdot\mathrm{kg}^{-1}\cdot\mathrm{K}^{-1} = A_0 t^{-\alpha} + A_1 t^{\Delta-\alpha} + A_2 + A_3 t + A_4 t^2 \tag{8}$$

where $\alpha = 0.112$ and $\Delta = 0.5$ are universal critical exponents; A_i's are non-universal adjusting constants. The values of the constants are given in Table IV for two- and one-phase vapor and liquid isochoric heat capacities at saturation.

5. CONCLUSIONS

The results of the isochoric heat capacity measurements of nitrogen tetroxide in the temperature range from 261.74 to 431.072 K, at densities between 201.21 and 1426.5 $\mathrm{kg}\cdot\mathrm{m}^{-3}$ using a high-temperature, high-pressure adiabatic calorimeter are presented. These measurements were made in the two-phase region along 26 isochores (15 liquid and 11 vapor densities) including along the coexistence curve and in the critical region. The results of the saturated density measurements are in satisfactory agreement with values derived from PVT measurements by other authors. Uncertainties of the measurements are estimated to be within 2%. The original C_V data were converted to the *ITS-90*. The liquid and vapor two-phase isochoric heat capacities, temperatures, and saturation densities were extracted from experimental data for each measured isochore. At temperatures around 351 K, the experimental two-phase C_V vs. specific volume V isotherms showed changes in the sign of the slope. The second temperature derivatives of both vapor pressure and chemical potential derived from measured two-phase isochoric heat capacities values increase sharply as the critical point is approached.

ACKNOWLEDGMENTS

The authors thank J. W. Magee for many valuable discussions during this work and for valuable remarks which improved the quality of the representations experimental data. One of us (I.M.A.) also thanks the Physical and Chemical Properties Division of the National Institute of Standards and Technology for the opportunity to work as a Guest Researcher at NIST during the course of this research. This work was also supported by Grant RFBR 00-02-17856.

REFERENCES

1. R. D. McCarty, H.-U. Steurer, and C. M. Daily, *The Thermodynamic Properties of Nitrogen Tetroxide*. National Bureau of Standards, NBSIR 86-3054 (1986).
2. V. B. Nesterenko, V. P. Bubnov, Yu. G. Kotelevskii, N. Ya. Lantratova, M. N. Mal'ko, A. M. Sukhotin, and B. D. Timofeev, *Physical and Chemical and Thermophysical Properties of Chemically Reacting System* (Minsk Science and Technology, 1976).
3. M. E. Fisher and G. Orkoulas, The Yang–Yang anomaly in fluid criticality: Experimental and scaling theory, in preparation.
4. G. Orkoulas, M. E. Fisher, and C. Ustün, The Yang–Yang relation and specific heats of propane and carbon dioxide, submitted to *J. Chem. Phys.*
5. T. J. Bruno and G. S. Straty, *J. Res. NBS* **91**:135 (1986).
6. G. C. Straty, A. M. F. Palavra, and T. J. Bruno, *Int. J. Thermophys.* **7**:1077 (1986).
7. Kh. I. Amirkhanov, N. G. Polikhronidi, B. G. Alibekov, and R. G. Batyrova, *Vesti AN BSSR, ser. Fizika-Energet. Nauk* **4**:113 (1981).
8. Kh. I. Amirkhanov, N. G. Polikhronidi, B. G. Alibekov, and R. G. Batyrova, *Thermophysical Properties of Substances at Condensed State* (Makhachkala, Dagestan FAN SSSR, 1982), p. 3.
9. N. G. Polikhronidi, R. G. Batyrova, and I. M. Abdulagatov, submitted to *Fluid Phase Equil.*
10. C. N Yang and C. P. Yang, *Phys. Rev. Lett.* **13**:303 (1969).
11. Kh. I. Amirkhanov, N. G. Polikhronidi, B. G. Alibekov, and R. G. Batyrova, *Teploenergetika* **12**:59 (1971).
12. Kh. I. Amirkhanov, G. V. Stepanov, and B. G. Alibekov, *Isochoric Heat Capacity of Water and Steam* (Amerind, New Delhi, 1974).
13. I. M. Abdulagatov, N. G. Polikhronidi, and R. G. Batirova, *J. Chem. Thermodyn.* **26**:1031 (1994).
14. I. M. Abdulagatov, N. G. Polikhronidi, and R. G. Batirova, *Ber. Bunsenger. Phys. Chem.* **98**:1068 (1994).
15. I. M. Abdulagatov, V. I. Dvoryanchikov, and L. G. Abramova, *J. Sol. Chem.* **28**:871 (1999).
16. N. B. Vargaftik, *Handbook of Physical Properties of Liquids and Gases*, 2nd ed. (Hemisphere, New York, 1983).
17. A. Pruss and W. Wagner, *Release on the IAPWS Formulation 1995 for the Thermodynamic Properties of Ordinary Water Substance for General and Scientific Use* (Frederica, Denmark, 1996).
18. Ya. R. Chashkin, V. A. Smirnov, and A. V. Voronel, *Thermophys. Prop. Substances Mater.* **2**:139 (1970).

19. A. V. Voronel, *Phase Transitions and Critical Phenomena*, C. Domb and M. S. Green, eds. (Academic Press, London, 1974), Vol. 5, p. 343.
20. I. M. Abdulagatov, L. N. Levina, Z. R. Zakar'yaev, and O. N. Mamchenkova, *Fluid Phase Equil.* **127**:205 (1997).
21. I. M. Abdulagatov and V. A. Dvoryanchikov, *J. Chem. Eng. Data* **43**:830 (1998)
22. A. Zh. Grebenkov, V. P. Zurbelev, A. B. Verzhinskaya, and V. B. Nesterenko, *Termophys. Prop. Substances Mater.* **27**:41 (1989).
23. R. L. Rosby, *J. Chem. Thermodyn.* **23**:1153 (1991).
24. A. Mittaseh, E. Kuss, and H. Z. Schlueter, *Anorg. Allg. Chem.* **159**:1 (1926).
25. H. H. Reamer and B. H. Sage, *Ind. Eng. Chem.* **44**:185 (1952).